Extraordinarily Large Optical Cross Section for Localized Single Nanoresonator

Ming Zhou, Lei Shi, Jian Zi, and Zongfu Yu

Phys. Rev. Lett. **115**, 023903 — Published 10 July 2015

DOI: 10.1103/PhysRevLett.115.023903

Extraordinarily Large Optical Cross Section for Localized Single Nanoresonator

Ming Zhou[1], Lei Shi[2,3], Jian Zi[2,3], and Zongfu Yu[1]

1. Department of Electrical and Computer Engineering, University of Wisconsin, Madison WI 53705, U.S.A.
2. Department of Physics, Key Laboratory of Micro- and Nano-Photonic Structures (MOE), and State Key Laboratory of Surface Physics, Fudan University, Shanghai 200433, China
3. Collaborative Innovation Center of Advanced Microstructures, Nanjing University, Nanjing 210093, China

Abstract: Using optical nanoresonator to realize extreme concentration of light at subwavelength nanoscale dimensions is of both fundamental and practical significance. Unfortunately, the optical cross section of an isotropic nanoresonator is determined by the resonant wavelength, which unfavorably limits the highest concentration ratio. Here we show that the cross section of a localized subwavelength resonator can be drastically enhanced, exceeding the size of wavelength by more than 3 orders of magnitude. A single microscopic nanoresonator could exhibit a macroscopic optical cross section. We further show that the enhancement can be implemented in simple dielectric structures that are readily compatible with optoelectronic integration. The giant optical cross section of a nano-object provide a versatile platform to create extremely strong light-matter interactions at nanoscale.

Concentrating light into sub-wavelength dimensions is of great importance to many applications that require strong light-matter interactions, such as ultra-fast photodetectors [1], single molecule fluorescence imaging [2], and Raman spectroscopy [3]. Optical nanoresonators have been known as an effective way to concentrate light into sub-wavelength dimensions [4]. The concentration performance can be evaluated by the ratio between the optical cross section and the geometrical size of a nanoresonator. Thus, there are mainly two routes to improve the concentration ratio. The first is to reduce the size of the resonator. Rapid progress has been made in this direction. For example, emerging two-dimensional and plasmonic materials have shown great potentials for deep sub-wavelength resonators, which could lead to extreme concentration of light and improved optoelectronic performance [1,4–7]. However, the fundamental trade-off between field confinement and optical loss is likely to limit the smallest size of a useful resonator. The second route is to increase the optical cross section of nanoresonators. The progress in this direction has been staggered. The maximum cross section remains about the same regardless of the construction of a subwavelength nanoresonators. It is around a few hundreds of nanometers in the visible spectral range for almost all resonators, including metallic nanoparticles, semiconductor nanowires, graphene resonators and plasmonic slit resonators [8–11]. Limited cross section has unfavorably limited the highest concentration ratio. Thus, to drastically enhance the cross section represents an exciting opportunity towards unprecedented light concentration and extremely strong light-matter interactions, particularly when it is combined with deep sub-wavelength nanoresonators.

However, the maximum optical cross section of a single nanoresonator is fundamentally limited by the resonant wavelength λ_0. A nanoresonator with an isotropic angular response has a maximum absorption cross-section of

$$\sigma_0 = \lambda_0^2/4\pi \tag{1}$$

We will refer Eq. (1) as the isotropic limit, which has been known for long time for the optical cross section of electronic transitions in atoms. Very recently, Eq. (1) was also explicitly shown for arbitrary dielectric and plasmonic nanoresonators [12,13].

Tremendous research efforts have been devoted to overcoming the isotropic limit. For example, Ruan and Fan recently [14] suggested using almost-degenerate plasmonic modes in a narrow spectral range to achieve super-scattering of nanoparticles, *i.e.* large scattering optical cross sections. However, this approach is fundamentally limited by the number of degenerate plasmonic modes. It hardly reaches a cross section greater than $10\,\sigma_0$. On the other hand, it is also well understood that restricting the angular distribution of the resonator's radiation can enhance the cross section. For example, a resonator with a dipolar radiation profile has a cross section of $1.5\,\sigma_0$ [12]. Polman, *et. al* [15] also recently showed that selectively exciting the local current in a nanoresonator can modify the angular response and thus enhance the cross section. However, the angular engineering approach is also limited to a few times of enhancement, unless an extended resonator with a size significantly larger than the wavelength is used [8,12]. All existing approaches can only achieve moderate enhancement ($< 10\,\sigma_0$). In addition, they have to rely on unique construction of nanoresonators and thus are not generally applicable for an arbitrary resonator.

In this Letter, we show that an extraordinarily large optical cross section of >1000 σ_0 could be achieved for a single sub-wavelength nanoresonator by embedding it in a material with a near-zero index. The enhancement does not require any specific construction of the nanoresonators and thus works for any nanoresonator. Most importantly, it can be realized in simple dielectric structures that are readily compatible with optoelectronic integration.

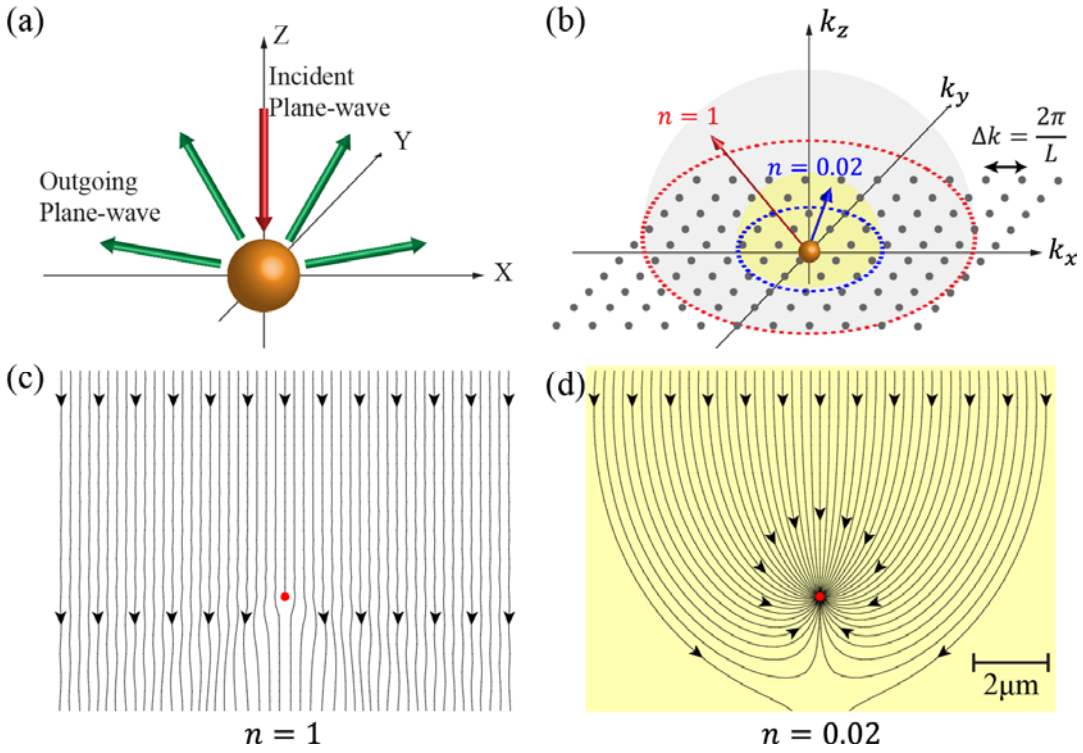

Fig. 1 (a) A resonator is excited by incident plane-wave (red arrow) and scatters light to other plane waves (green arrows). (b) Channels are represented by the dots in the projected k_{xy}-space. More coupling channels are available in vacuum as enclosed in the grey sphere (n = 1) than in index near-zero materials as enclosed in the yellow sphere (n = 0.02, not drawn to the scale) (c-d) Flow of the Poynting vectors around a nanoresonator in vacuum (c) and index near-zero material (d). The resonator (red circle) has a radius of 0.1 μm.

To understand the mechanism of the cross section enhancement, we first briefly review how the conventional approach works based on the restriction of the angular response of a nanoresonator. For concreteness, we focus on the absorption cross section. The scattering cross section can be understood similarly. Fig. 1(a) shows the schematic of a continuous space containing a single nanoresonator. When excited by a plane-wave illumination, photons couple into the nanoresonator. At the same time, resonantly stored photons in the nanoresonator also couple to plane waves in many other directions, which is the scattered light. The balance of in- and out-coupling of photons determines the light absorption in the nanoresonator. It can be easily shown by a coupled-mode theory that the fewer channels the nanoresonator couples to, the more the absorption and the larger the cross section is [16]. The angle-restriction method works by carefully arranging the field distribution in the nanoresonator such that it decouples from certain channels. As a result, the radiation pattern exhibits a narrower angular distribution and the absorption cross section is enhanced above the isotropic limit σ_0. The decoupling is typically created by symmetry or cancellation of field overlap integral. As such, this method does not

work well for sub-wavelength nanoresonators because it is difficult to cancel the coupling to many directions by arranging the fields within a small spatial size.

Instead of relying on specially designed nanoresonators to decouple channels, here we directly reduce the number of channels by filling the entire space with an index near-zero material. Such material has lower density of channels than vacuum. To see such difference, we first introduce a method for quantifying the channels in a continuous free space. Each plane wave in a free space defines a channel characterized by its unique wave vector. There are always infinitely many channels in a continuous free space regardless its index. To overcome this infinity, we adopt a mathematical treatment that is often referred as box quantization. First, one starts by considering a free space with a lateral periodicity of L in x and y direction. Then, one can take the limit of $L \to \infty$ [12,16] to recover the case of infinitely large free-space. For a given L, the number of channels is finite and they can be represented in the k-space as shown in Fig. 1(b). Channels are evenly distributed and spaced by $\Delta k = 2\pi/L$. All coupling channels are located on a sphere with a radius $k_0 = n\omega_0/c$, where ω_0 is the resonant frequency and n is the refractive index of the continuum. They can also be represented in the projected k_{xy}-space. It is evident that the total number of channels is determined by the radius k_0, which is linearly proportional to refractive index n. In common dielectrics where $n > 1$, there are more channels available than in vacuum, resulting in cross sections smaller than σ_0. On the other hand, in an index near-zero material, $n \sim 0$ and the number of channels reduces below that in vacuum (yellow sphere in Fig. 1(b)), resulting in enhanced cross section.

The above prediction can be rigorously proved using a free-space coupled-mode theory developed in [12]. Here we go through the main results and leave the details to the Supplementary Material. The amplitude of photon energy in the nanoresonator can be represented by a, which is normalized such that $|a|^2$ represents the energy. The amplitude of the flux of incoming and outgoing plane waves are described by two N-dimensional vectors $\mathbf{S_{in}}$ and $\mathbf{S_{out}}$, respectively, where $N = 2\pi \lfloor nL/\lambda_0 \rfloor^2$ is the total number of channels. The floor operator $\lfloor A \rfloor$ gives the largest integer smaller than A. The total coupling rate and the intrinsic absorption rate are γ_c and γ_a, respectively. The coupled-mode equations are

$$\frac{d}{dt}a = j\omega_0 a - \frac{\gamma_a}{2}a - \frac{\gamma_c}{2}a + \boldsymbol{D^T}\mathbf{S_{in}} \tag{2}$$

$$\mathbf{S_{out}} = \boldsymbol{C}\mathbf{S_{in}} + a\boldsymbol{D} \tag{3}$$

The N-dimensional vector $\boldsymbol{D}$ describe the coupling rate to each channel and $\boldsymbol{D^+D} = \gamma_c$. For an isotropic resonator, the element of $\boldsymbol{D}$ is given by $\gamma_i = \gamma_c/(2Ncos\theta_i)$, where θ_i is the polar angle associated to the channel i. The $N \times N$ scattering matrix $\boldsymbol{C}$ describes the direct transmission between the incoming and outing waves. It satisfies [17] $\boldsymbol{CD}^* = -\boldsymbol{D}$. The absorption cross-section then can be calculated in the frequency domain as

$$\begin{aligned}\sigma &= \frac{\mathbf{S_{in}^*}\mathbf{S_{in}} - \mathbf{S_{out}^*}\mathbf{S_{out}}}{\mathbf{S_{in}^*}\mathbf{S_{in}}/(L^2cos\theta_i)} = \frac{1}{\mathbf{S_{in}^*}\mathbf{S_{in}}/(L^2cos\theta_i)}\frac{\gamma_a\mathbf{S_{in}^*}\boldsymbol{D}^*\boldsymbol{D^T}\mathbf{S_{in}}}{(\omega-\omega_0)^2 + (\frac{\gamma_a}{2}+\frac{\gamma_c}{2})^2} \\ &= \frac{1}{4\lfloor nL/\lambda_0 \rfloor^2 \pi}\frac{\gamma_a\gamma_c}{(\omega-\omega_0)^2 + (\frac{\gamma_a}{2}+\frac{\gamma_c}{2})^2}L^2\end{aligned} \tag{4}$$

In the limit of $L \to \infty$, the floor operator can be dropped out. We obtain

$$\sigma = \frac{\lambda_0^2}{4\pi n^2} \frac{\gamma_a \gamma_c}{(\omega - \omega_0)^2 + (\frac{\gamma_a}{2} + \frac{\gamma_c}{2})^2} \tag{5}$$

At the resonant wavelength and with a critical coupling condition $\gamma_a = \gamma_c$, the maximum absorption cross section is

$$\sigma_{3D} = \frac{\lambda_0^2}{4\pi n^2} = \frac{\sigma_0}{n^2} \tag{6}$$

In an index near-zero medium with $n \sim 0$, an extraordinary large absorption cross section can be obtained as shown in Eq. (6). Similarly, in a 2-dimensional (2D) space, the limit of absorption cross-section can be obtained as $\sigma_{2D} = \frac{\lambda_0}{2\pi n}$.

The enhancement of optical cross section can also be easily shown by numerically solving Maxwell's equations for a nanoresonator. Figure 1(c-d) compares the power flow of a plane wave illuminated on a nanoresonator in vacuum (n = 1) and in a near-zero index material (n = 0.02). The nanoresonator is an infinitely long dielectric rod with a radius of 100 nm and a refractive index of 4. The simulation is performed in 2D. The imaginary part of the refractive index of the nanoresonator is tuned to ensure the absorption cross section always reaches its maximum. The nanoresonator has a fundamental resonance at the wavelength of 1.05 μm. When placed in vacuum, its cross section reaches the 2D isotropic limit $\sigma_{2D\_0} = 0.16$ μm. The flux lines are only disturbed around the nanoresonator itself as shown in Fig. 1(c). In great contrast, in a near-zero index material, the flux lines from a large area bend toward the resonator as shown in Fig. 1(d). The absorption cross-section is $\sigma_{2D\_n} = 8$ μm, which is 50 times of σ_{2D_0} and agrees very well with the analytical theory.

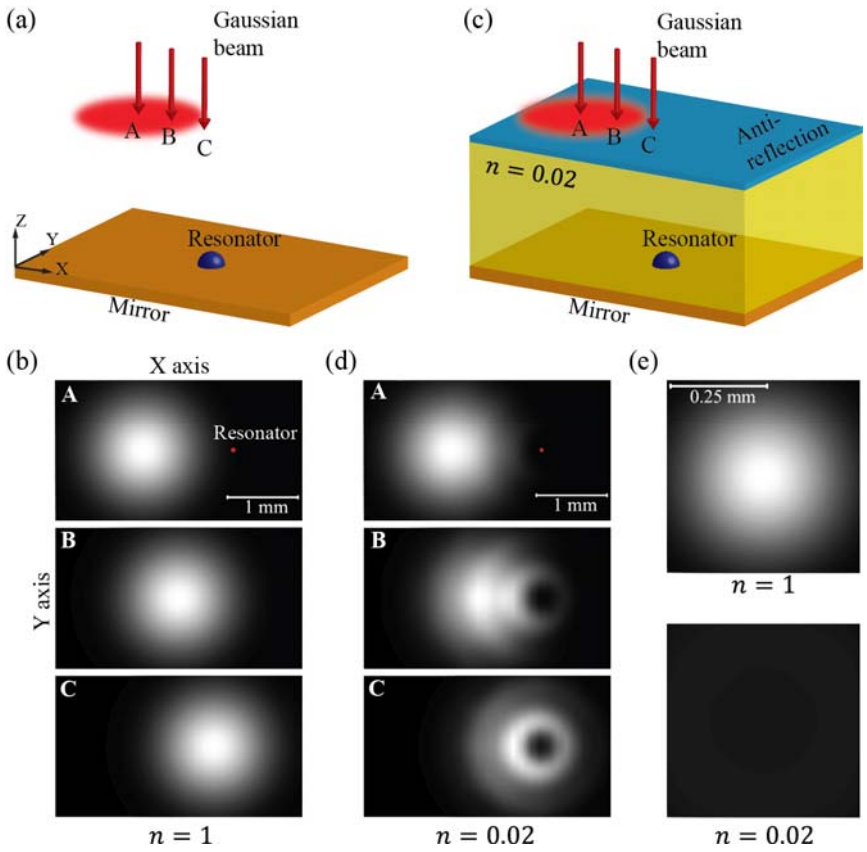

Fig. 2 (a) A Gaussian beam scans across a resonator placed on a perfect mirror in vacuum. (b) The top view of the spatial intensity of the reflected beam measured at three different positions A, B, and C (also labeled in (a)). Red dot indicates the position of the resonator. (c) Similar to (a), but the resonator is in a slab of an index near-zero material. Anti-reflection layer is placed on the top of the slab to ensure that there is no external cavity formed by the slab. In both cases (a) and (c), the reflected beam profile is obtained at a fixed distance from the resonator. (d) Reflected beam profiles at three different positions A, B, and C. A macroscopic shadow created by an extraordinarily large cross section emerges in the reflected beam profile. (e) Top panel: A matching Gaussian beam with a waist that is same as the size of the shadow in (d). Bottom panel: the reflected beam when shining on the resonator in the index near-zero material. The beam is completely absorbed.

The enhancement for the same index of n = 0.02 is even greater for the 3-dimensional (3D) case, where the enhancement factor $1/n^2$ reaches 2500. Such an extraordinary enhancement could lead to macroscopic cross sections for microscopic nanoresonators. We can visualize the cross section based on the response of the resonator under a Gaussian illumination. Fig. 2(a) shows the setup where a Gaussian beam with a waist of 1 mm scans around a resonator, which is placed on a perfect mirror and has a resonant wavelength of 10 μm. Such resonators typically have a size that is only a few micrometers. As expected, the reflected beam profile barely changes as it scans across the resonator (Fig. 2(b)). One cannot identify the presence of the nanoresonator because its maximum absorption cross section is only $\sigma_0 \cong 16 \times 10^{-6}\ \mathrm{mm}^2$, which corresponds to a circle with a radius of 2.3 μm.

If we embedded the resonator in an index near-zero slab with the same Gaussian illumination (Fig. 2(c)), the reflected beams (Fig. 2(d)) exhibit a macroscopic shadow with a diameter of 0.25 mm because of the extraordinarily large absorption cross section $\sigma \cong 0.064\ \mathrm{mm}^2$. To further

illustrate such giant cross sections, a matching Gaussian beam with a waist of 0.25 mm (upper panel in Fig. 2(e)) is used to illuminate the resonator. The beam is completely absorbed as shown by the lower panel in Fig. 2(e). The detailed method is described in the Supplementary Material.

In above analysis, we have assumed ideal index near-zero materials without specifying their implementation. Near-zero indices can be either realized by intrinsic material properties or by effective indices of structured medium. The proposed enhancement works for both. While the field of index near-zero materials is rapidly evolving [18,19] most current implementations either rely on lossy materials, or require complex nano-patterning of dielectric materials [20,21]. It is difficult to embed nanoresonators in these materials. Next, we describe a simple approach that can be readily implemented in common materials and structures based on external cavities.

It is important to recognize that one only needs a near-zero *phase* index in order to reduce the number of channels in the *k*-space. Phase index is the ratio between the wave vector in a medium and that in vacuum. Inset of Fig. 3(a) shows a two-mirror structure where the phase index approaches zero near the band edge of the fundamental mode (Fig. 3(a)). The number of channels between the mirrors greatly decreases at the band edge. From a microscopic point of view, the reflection at the mirrors causes destructive interference that removes many channels in-between the mirrors. Such an effective index near-zero material has also been studied to enhance the spontaneous emission [22–24] and cavity quantum electrodynamics [25].

We then place a nanoresonator inside two mirrors. The resonant wavelength $\lambda_0 = 2d$ is chosen such that it overlaps with band edge. The analytical derivation of the absorption cross section is shown in the Supplementary Material. The effective index can be calculated as

$$n_{eff} = \frac{1}{\sqrt{2}} \frac{1-|r|}{|t|} \tag{7}$$

Here *r*, *t* are the reflection and transmission coefficient of the top mirror.

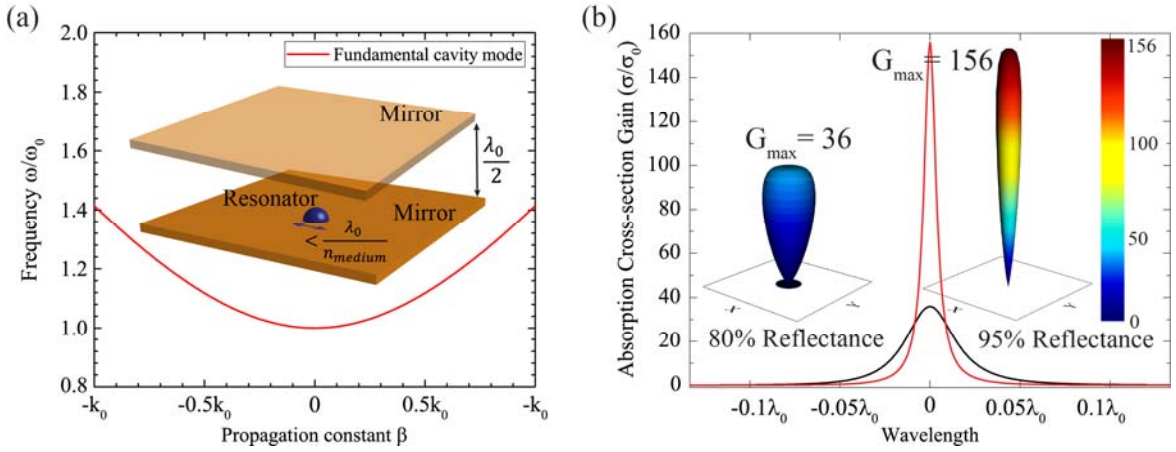

Fig 3. (a) Schematic of the near-zero phase index structure consisting of two mirrors. The dispersion curve is obtained assuming the mirror has 100% reflection. (b) The spectral of the absorption cross-section for mirrors with 80% (black solid line) and 95% (red solid line) reflectance. Insets show the angular response for both cases.

For a top mirror with an 80% reflectance (Fig. 3(b)), $n_{eff} = 0.167$ and the maximum absorption cross section is enhanced by 36 times compared to the isotropic limit σ_0. For a reflectance of 95%, $n_{eff} = 0.08$, and the maximum cross-section further increases to 156 σ_0. As the reflectance increases, the bandwidth decreases because fewer channels lead to weaker coupling rates. At the same time, the angular responses become more anisotropic (insets in Fig. 3(b)) with more absorption in the normal direction and less in off-normal directions.

Lastly, we use numerical simulations to directly validate the two-mirror design. An isotropic 2D resonator is formed by a nano slit in a perfect electric conductor (PEC) (Fig. 4(a)), which has a resonant wavelength at $\lambda_0 = 1570$ nm. The top mirror is a Distributed Bragg Reflector (DBR) consisting of 3 pairs of Si and SiO_2 quarter-wave layers. The DBR has a peak reflectance of 98%. A finite difference method is used to numerically solve the frequency domain (FDFD) Maxwell's equations in a total-field scattered-field configuration. The isotropic limit is $\sigma_{2D} = \lambda_0/2\pi = 250$ nm while the simulated absorption cross section shows almost 24-fold enhancement and reaches 5900 nm (Fig. 4(b)). Independent of the numerical simulation, we also calculate the spectrum based on the coupled-mode theory without any fitting parameters. The reflection and transmission coefficients of the DBR mirror are directly calculated through transfer matrix method. The absorption rate γ_a is calculated by [12] $\gamma_a = 2n_i/n_r\omega_0$, where n_i and n_r are the imaginary and real part of the refractive index of the material in the slit, respectively. The coupled-mode theory (red solid line Fig. 4(b)) shows remarkable agreement with the direct simulation despite the fact that the spectral line shape is no longer Lorentzian. The detailed derivation of 2D coupled-mode theory is available in the Supplementary Material. To further verify the predicted anisotropic angular response, Fig. 4(c) shows the scattered field of the nanoresonator without (top panel) and with (bottom panel) the top mirror. Indeed, the scattered fields become much more directional once the resonator is placed in a phase index near-zero structure.

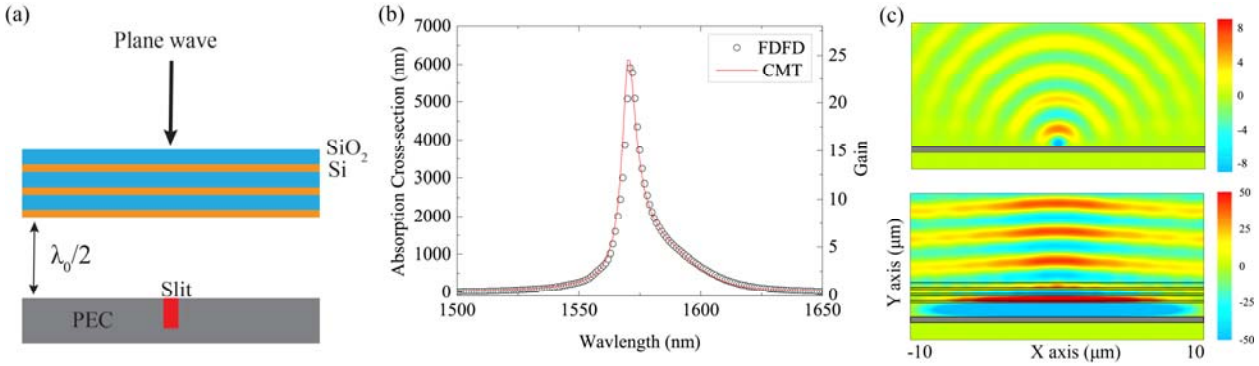

Fig.4 (a) Schematic of the 2D numerical simulation. The resonator is formed by a nano slit on a PEC slab. The depth and width of the slit is 110 nm and 20 nm, respectively. The slit is filled with dielectric material, which has a refractive index of 3.5-*j*0.07. The spacing between PEC and the DBR is 785 nm. (b) Simulated absorption cross-section spectrum (circles) agrees very well with the coupled-mode theory (solid line). (c) The scattered fields from the nanoresonator without (upper) and with (lower) the top mirror.

In conclusion, we theoretically demonstrate that the optical cross section of a single localized nanoresonator can be drastically enhanced in phase index near-zero materials. The light

concentration effect is completely different from conventional lenses systems, where the location of the light concentration is always fixed at the focus point. Here light is always concentrated on the nanoresonator regardless of its position, providing a versatile platform to create extremely strong light-matter interactions at the nanoscale.

Acknowledgement: The work was supported by the Wisconsin Alumni Research Foundation and the Office of Naval Research under grant number N00014-14-1-0300.

Reference:

[1] L. Tang, S. E. Kocabas, S. Latif, A. K. Okyay, D.-S. Ly-Gagnon, K. C. Saraswat, and D. A. B. Miller, Nat. Photonics **2**, 226 (2008).
[2] A. Kinkhabwala, Z. Yu, S. Fan, Y. Avlasevich, K. Müllen, and W. E. Moerner, Nat. Photonics **3**, 654 (2009).
[3] X. Qian, X.-H. Peng, D. O. Ansari, Q. Yin-Goen, G. Z. Chen, D. M. Shin, L. Yang, A. N. Young, M. D. Wang, and S. Nie, Nat. Biotechnol. **26**, 83 (2008).
[4] J. A. Schuller, E. S. Barnard, W. Cai, Y. C. Jun, J. S. White, and M. L. Brongersma, Nat. Mater. **9**, 193 (2010).
[5] E. Prodan, C. Radloff, N. J. Halas, and P. Nordlander, Science **302**, 419 (2003).
[6] L. Novotny and N. van Hulst, Nat. Photonics **5**, 83 (2011).
[7] M. I. Stockman, Opt. Express **19**, 22029 (2011).
[8] Z. Yu, G. Veronis, S. Fan, and M. L. Brongersma, Appl. Phys. Lett. **89**, 151116 (2006).
[9] L. Cao, J. S. White, J.-S. Park, J. A. Schuller, B. M. Clemens, and M. L. Brongersma, Nat. Mater. **8**, 643 (2009).
[10] P. Fan, Z. Yu, S. Fan, and M. L. Brongersma, Nat. Mater. **13**, 471 (2014).
[11] S. Yi, M. Zhou, X. Shi, Q. Gan, J. Zi, and Z. Yu, Opt. Express **23**, 10081 (2015).
[12] L. Verslegers, Z. Yu, P. B. Catrysse, and S. Fan, J. Opt. Soc. Am. B **27**, 1947 (2010).
[13] Z. Ruan and S. Fan, Phys. Rev. A **85**, 043828 (2012).
[14] Z. Ruan and S. Fan, Phys. Rev. Lett. **105**, 013901 (2010).
[15] T. Coenen, F. Bernal Arango, A. Femius Koenderink, and A. Polman, Nat. Commun. **5**, (2014).
[16] Z. Yu, A. Raman, and S. Fan, Proc. Natl. Acad. Sci. **107**, 17491 (2010).
[17] W. Suh, Z. Wang, and S. Fan, IEEE J. Quantum Electron. **40**, 1511 (2004).
[18] A. Alù, M. G. Silveirinha, A. Salandrino, and N. Engheta, Phys. Rev. B **75**, 155410 (2007).
[19] S. Molesky, C. J. Dewalt, and Z. Jacob, Opt. Express **21**, A96 (2013).
[20] X. Huang, Y. Lai, Z. H. Hang, H. Zheng, and C. T. Chan, Nat. Mater. **10**, 582 (2011).
[21] P. Moitra, Y. Yang, Z. Anderson, I. I. Kravchenko, D. P. Briggs, and J. Valentine, Nat. Photonics **7**, 791 (2013).
[22] P. Goy, J. M. Raimond, M. Gross, and S. Haroche, Phys. Rev. Lett. **50**, 1903 (1983).
[23] C. B. Poitras, M. Lipson, H. Du, M. A. Hahn, and T. D. Krauss, Appl. Phys. Lett. **82**, 4032 (2003).
[24] R. Sokhoyan and H. A. Atwater, Opt. Express **21**, 32279 (2013).
[25] K. J. Vahala, Nature **424**, 839 (2003).